Room-Temperature 2-D X-Ray Imaging With the Controlled-Drift Detector

Andrea Castoldi, *Member, IEEE*, Giuseppe Cattaneo, Antonio Galimberti, Chiara Guazzoni, *Member, IEEE*, Pavel Rehak, *Member, IEEE*, and Lothar Strüder

***Abstract*—The controlled-drift detector is a single-photon counting X-ray imaging silicon detector that features excellent energy and time resolution. Its distinctive feature is the readout of the signal charge packets stored in each pixel column by means of an electrostatic field in few μs. The drift time of the charge packet identifies the pixel of incidence. Several one-dimensional flat images of single pixel columns have been acquired to investigate the achievable position resolution and the improvement of the energy resolution at high frame rates (up to 125 kHz). At 62.5 kHz, the room-temperature energy resolution at the Mn Kα line is better than 300 eV full-width at half-maximum. The first two-dimensional X-ray images of different masks carried out at frame frequencies in the range 10-100 kHz, both with radioactive and synchrotron light sources, will be presented.**

***Index Terms*—Controlled-drift detector, fast readout, X-ray imaging, X-ray radiograph.**

I. Introduction

THE controlled-drift detector (CDD) [1], [2] is a fully depleted silicon detector that allows two-dimensional (2-D) position sensing, energy spectroscopy of X-rays in the range 0.5–30 keV, and an unprecedented time resolution. It was proposed in 1997 [3]. The first experimental evidence of its working principle was reported in [4].

The basic structure of the CDD is constituted by a thick high-resistivity n-type substrate on which a thinner lower resistivity n-type epitaxial layer has been grown. The n^+ collecting anodes and the p^+ field strips are implanted on the top of the epitaxial layer. The p^+ layer(s) implanted on the bottom of the substrate is used as the entrance window of the X-rays. The technology used for the entrance window allows one to obtain a quantum efficiency higher than 80% at the carbon line (282 eV) and 85% at the oxygen line (523 eV) [5]. The limitation in the detector quantum efficiency at higher energies arises from the detector thickness. With the present prototype (300 μm thick), the detector quantum efficiency is about 90% at 10 keV and still 9% at 30 keV. The use of a 500-μm-thick substrate improves to 14% the quantum efficiency at 30 keV. The n^+ collecting anodes, the field strips, and the uniform back contact are biased in such a way as to fully deplete the wafer and to have the drifting channel for the signal electrons within the epitaxial layer (see Fig. 1).

The CDD is operated in integrate-readout mode, like a charge-coupled device [5]. During the integration phase, the signal electrons generated by the incident X-ray are stored in suitably engineered potential wells in spite of a superposed drift field. During the readout (or drift) phase, an external control voltage smooths the potential wells out so that the drift field is free to transport the signal electrons to the readout electrode. To achieve this, the p^+ field strips are biased with suitable voltages that are static during each phase but different for integration and readout, as shown in the inset of Fig. 1. Properly designed regions of channel-stop implants prevent the broadening of the signal charge along the direction transversal to the drift.

When operated in integrate-readout mode, the CDD is inherently faster than the charge-coupled device, based on the clocked transfer of the rows of pixels toward the readout section. Drift velocities in the range 0.2–0.5 cm/μs have been measured and should lead to readout times on the order of 3–5 μs for a 1-cm-long detector. The fast transport mechanism allows short integration times and is the key to obtain room-temperature energy resolution close to that obtainable with state-of-the-art X-ray imagers typically operating at cryogenic temperatures and lower frame frequency.

In this paper, we present the characterization of a CDD prototype at room temperature, with particular emphasis on 2-D X-ray imaging and spectroscopy. In Section II, we present the flat images of a ^{55}Fe source obtained with the CDD at different frame rates up to 125 kHz. In Section III, the first X-ray images of different masks carried out at frame frequencies in the range 10–100 kHz, with both radioactive and synchrotron light sources, will be presented.

II. 1-D X-ray Imaging and Spectroscopy

We mounted a CDD prototype with 2-mm drift length (11 pixels long) and four pixel columns (180 μm wide each). The operating drift field was 400 V/cm, and the amplitude of the surface perturbation was 2 V. All the measurements have been carried out at room temperature. The detector has been irradiated with a ^{55}Fe source to verify the imaging capability, the maximum frame rate, and the achievable energy resolution. The pulses delivered by the on-chip junction field-effect transistor (source follower configuration) of each pixel column were fed to a low-noise voltage preamplifier followed by a

Manuscript received November 24, 2001; revised March 11, 2002. This work was supported by the Istituto Nazionale di Fisica Nucleare—Sezione di Milano, by the Italian Space Agency, and by the U.S. Department of Energy under Contract DE-AC02-98CH10886.

A. Castoldi and G. Cattaneo are with the Dipartimento di Ingegneria Nucleare Ce.S.N.E.F., Politecnico di Milano, 20133 Milano, Italy, and INFN, Sezione di Milano, Milano, Italy (e-mail: Andrea.Castoldi@polimi.it).

A. Galimberti and C. Guazzoni are with the Dipartimento di Elettronica e Informazione, Politecnico di Milano, 20133 Milano, Italy, and INFN, Sezione di Milano, Milano, Italy (e-mail: Chiara.Guazzoni@mi.infn.it).

P. Rehak is with the Instrumentation Division, Brookhaven National Laboratory, Upton, NY 11973 USA (e-mail: rehak@bnl.gov).

L. Strüder is with the Halbleiterlabor, Max Planck Institut, D-81279 Munich, Germany (e-mail: lts@hll.mpg.de).

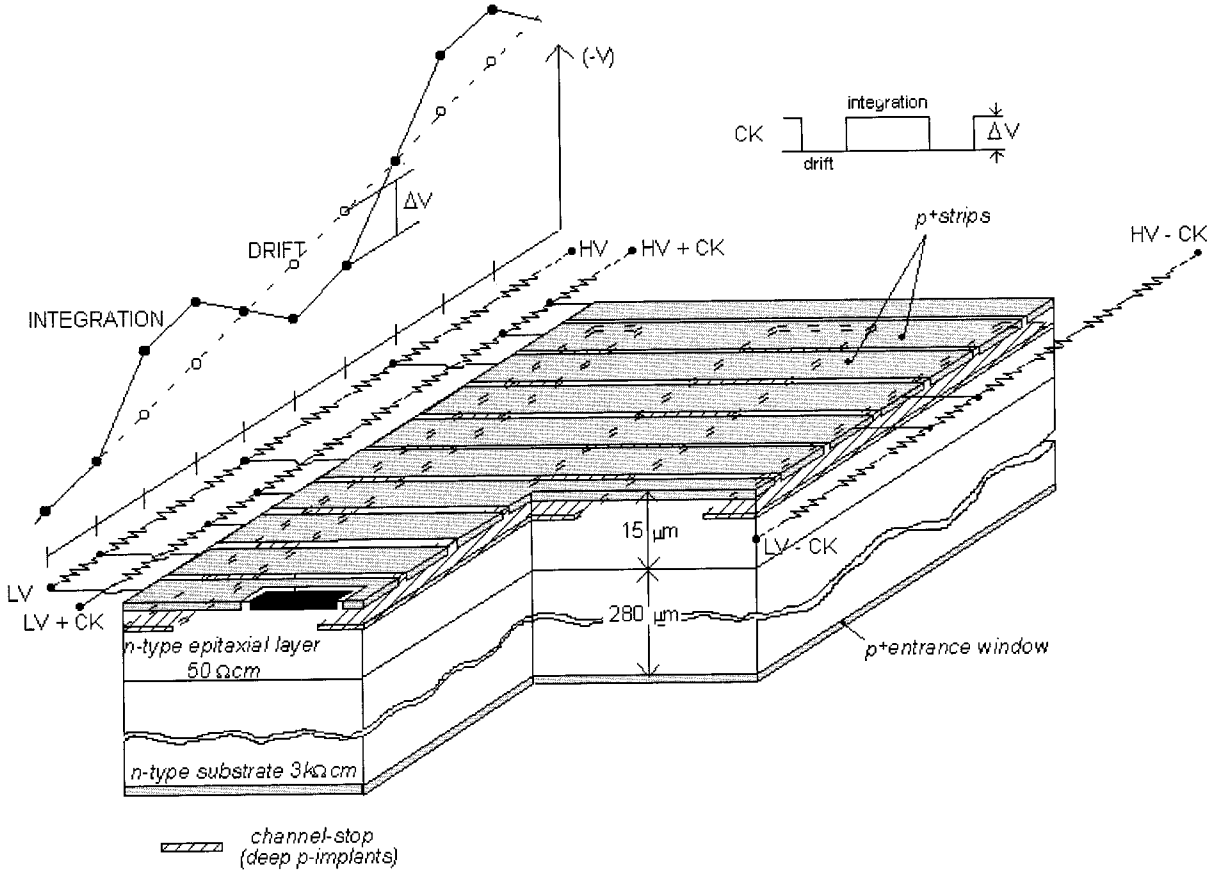

Fig. 1. View of the controlled-drift detector. The inset shows a diagram of the potential of the strips of the front side during the integration and the drift phases. Two channels are shown.

pseudo-Gaussian shaper (0.25μs shaping time) and an 8-bit digitizer controlled by a PC to acquire the output waveforms, subtract the background (mainly due to thermal generation), and compute the amplitude and the drift time of each pulse.

We acquired several one-dimensional (1-D) flat images for different frame rates. As the detector area is unshielded, the ratio between the integration time and the readout time is typically chosen much greater than one in order to limit the number of out-of-time events. In our case, it was set equal to nine in all the measurements. With this choice, we tested the CDD up to 125-kHz frame rate, corresponding to a duration of the drift phase of only 0.8μ s. As the electron drift occurs within the first 0.6μ s of the readout phase, for frame frequencies greater than 80 kHz signal processing overlaps with the subsequent integration phase.

Fig. 2 shows the scatter plot energy versus drift time (i.e., position) of the detected events detected by a single column when the CDD is operated at 100-kHz frame rate. Moving along the time axis, we see that the events are gathered in well-separated clusters centered at about 6 keV (the Mn Kα and Mn Kα lines can be clearly distinguished), indicating the illuminated pixels.

The upper inset of Fig. 2 shows the distribution of the events along the time axis. The FWHM of the peaks is about 20%, leaving a margin for reduction of the pixel size along the drift coordinate (actual size is 180 μm).

The inset on the right side of Fig. 2 shows the total distribution of the event energies (i.e., the spectrum of the ^{55}Fe source collected by all the pixels in the column). The energy resolution at the Mn Kα line (5.899 keV) is 277.5 eV FWHM, corresponding to an equivalent noise charge (ENC) of 29.6 electron rms.

A. "Virtual Cooling"

When operating an imager at room temperature, the main noise contribution generally arises from the leakage current that is integrated in the pixels during the integration time. This contribution can be reduced either by cooling the detector or by increasing the operating frequency of the detector. In fact, by increasing the frame frequency, we shorten the integration time and therefore reduce the amount of leakage charge that accumulates in the pixels, obtaining a "virtual cooling" effect. As the CDD can be operated at frame frequencies more than one order of magnitude higher than present state-of-the-art X-ray imagers, we expect a significant improvement in the achievable room-temperature energy resolution.

In Fig. 3, the squared ENC is reported as a function of the integration time. At 10-kHz frame rate, the ENC is 58.7 electrons rms, while at 125-kHz frame rate, the parallel noise contribution reduces to 28.4 electrons rms. According to the model discussed in [6], from the slope of the fit we get a leakage current of about 7.7 pA, corresponding to a leakage current density of about 2 nA/cm^2.

B. "Electronic Collimation"

As the CDD is a pixellated detector, the energy photopeak shows a shoulder at lower energies, as the generated charge

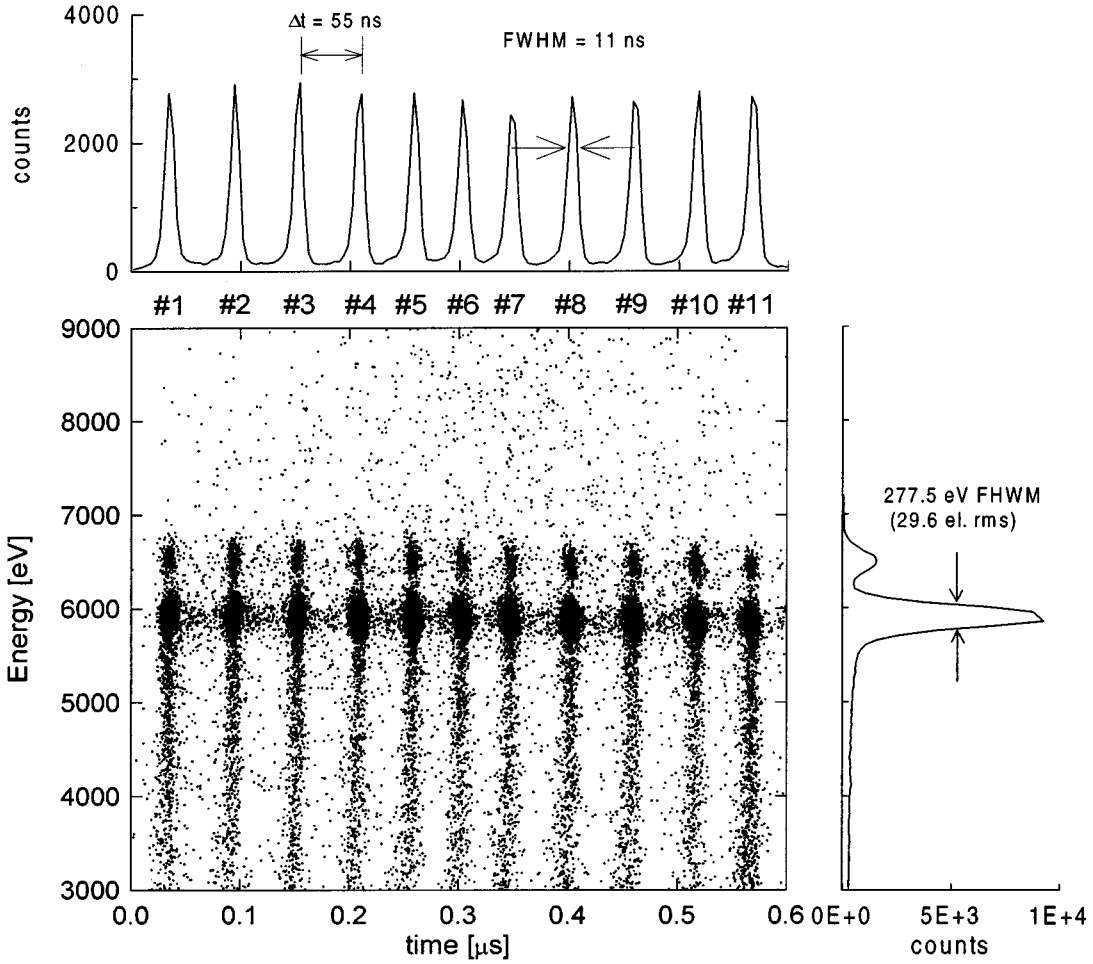

Fig. 2. Scatter plot energy versus drift time of the X-rays of a ^{55}Fe source collected by irradiating a column of the CDD at 100-kHz frame frequency. The integration time was set to 9 μs and the readout time to 1 μs. The upper inset shows the distribution of the events along the time axis. The inset on the right end shows the total distribution of the event energies (i.e., the spectrum of the ^{55}Fe source collected by all the pixels).

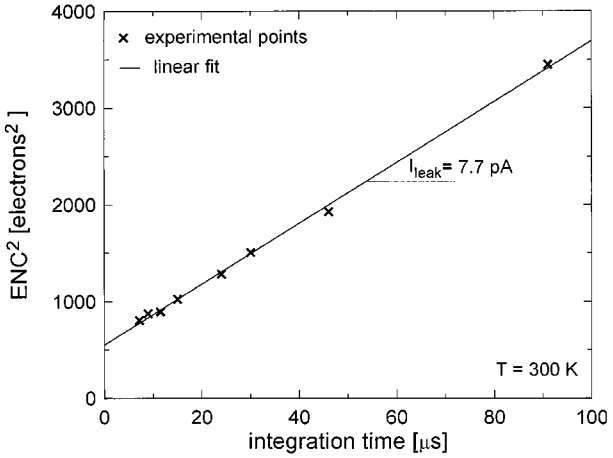

Fig. 3. Measured ENC^2 as a function of the integration time.

may be shared in more than one pixel. Different kinds of charge sharing can occur, as shown in Fig. 4(a). The charge cloud can be shared between two pixels of the same row and of neighbor columns (label A), giving rise to two pulses at channels n and $(n+1)$ having the same drift time but less energy than the photopeak. When the sharing occurs between two pixels of the same column and of two different rows (label B), the measured energy depends on the shaping time and the measured drift time is within the drift times of the two pixels. When the charge sharing occurs among four pixels of neighbor rows and columns (label C), the two pulses will have both an intermediate drift time and energy lower than the photopeak. In Fig. 4(b), we have highlighted the regions of the scatter plot where the charge-sharing events described above are located. We can identify and reject the events affected by sharing phenomena by postprocessing the acquired images. The obtained scatter plot is shown in Fig. 5. Apart from the first and last pixels that clearly include shared events between the anode and guard region, respectively, the other pixels show a marked reduction of the photopeak shoulder. The final result is equivalent to an "electronic collimation" of the incident radiation. Fig. 6 compares the energy spectrum of the events in Figs. 4(b) and 5. Thanks to the rejection of the shared events, the Si escape peak begins to appear. If we reject also the events collected in the first and in the last pixel, the peak-to-background ratio increases up to about 900 and the escape peak becomes more clearly visible.

III. 2-D X-Ray Imaging

A. Measurements With a Radioactive Source

To further probe the imaging capabilities of the CDD, 2-D X-ray images of different masks have been carried out at frame

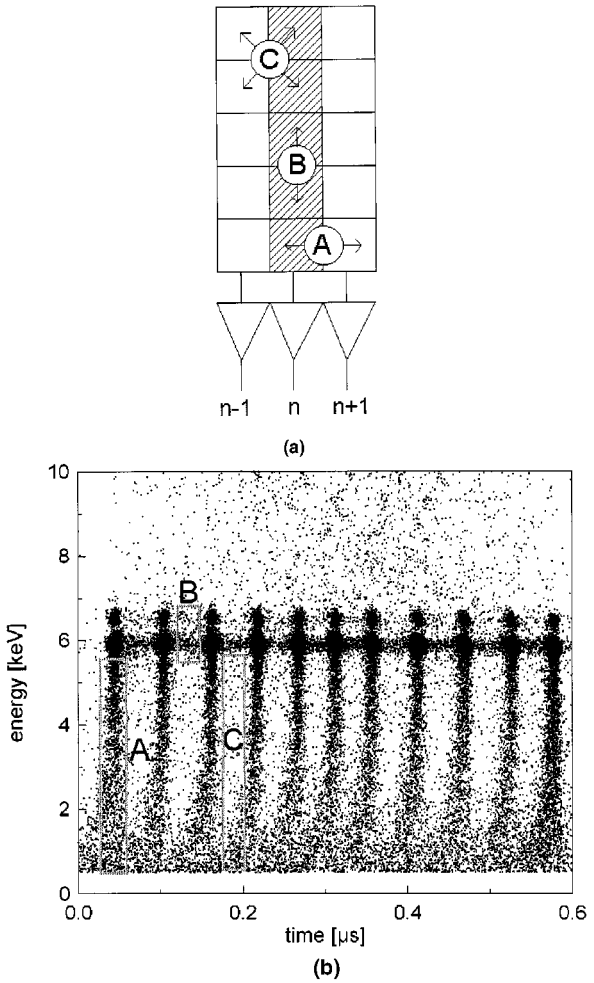

Fig. 4. (a) Scheme of principle of the possible charge-sharing phenomena. The charge cloud labeled C shares among four pixels, while those labeled A and B share only between two pixels. (b) Scatter plot energy versus drift time of the X-rays of a ^{55}Fe source collected by a column of the CDD at 100-kHz frame frequency. The rectangles show the regions where charge-sharing events are located.

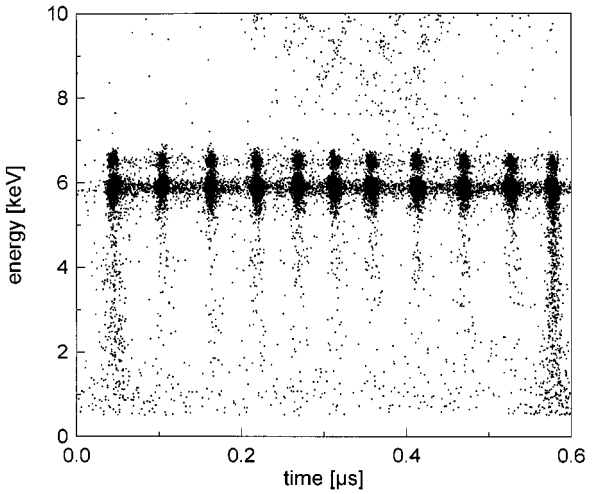

Fig. 5. Scatter plot energy versus drift time of the X-rays of a ^{55}Fe source collected by a column of the CDD at 100-kHz frame frequency once the events affected by sharing phenomena have been rejected.

frequencies in the range 10–100 kHz. A scheme of the principle of the experimental setup is shown in Fig. 7(a). A mask is

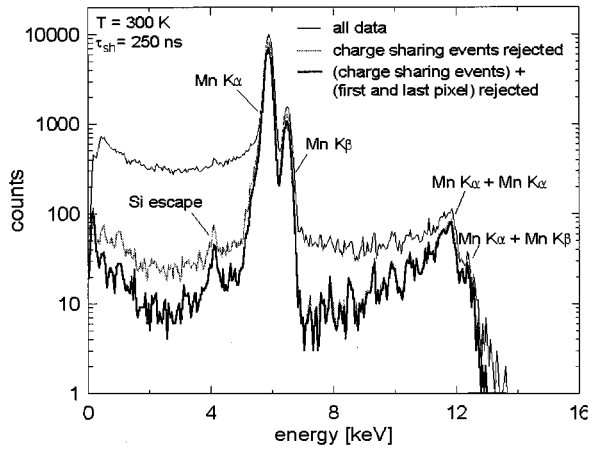

Fig. 6. Energy spectrum of the events in Fig. 4(b) (thin black line) and Fig. 5 (gray line). If we reject also the events collected in the first and last pixel, in part shared with the anode and the guard region, respectively (thick black line), the peak-to-background ratio doubles.

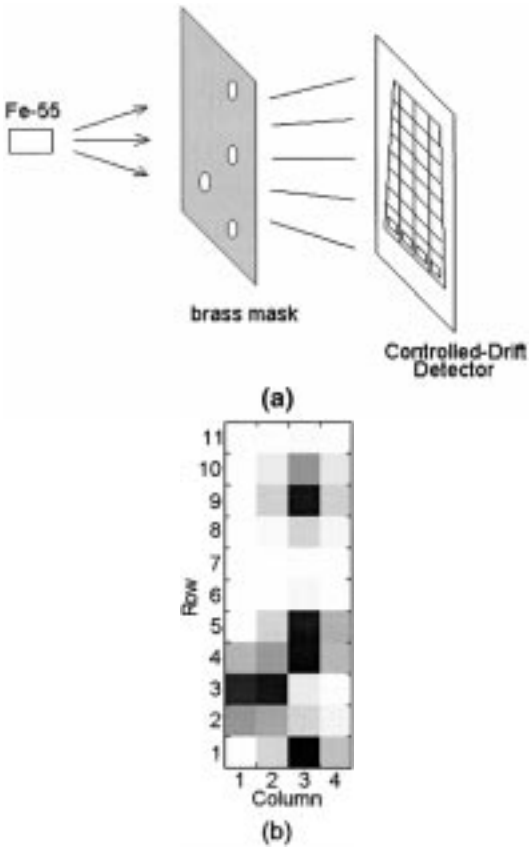

Fig. 7. (a) Scheme of principle of the experimental setup used for the measurement with a ^{55}Fe radioactive source. The hole's diameter is 0.2 mm. The hole distance is 0.4 mm in the vertical direction and 0.2 mm in the horizontal direction. The distance between the mask and the detector is 1.5 mm. (b) Raw data collected at room temperature by four columns of 11 pixels each. The CDD was operated at 10-kHz frame frequency.

inserted between the source and the detector. The transmitted image is recorded by the CDD. As the image is collected in single-photon counting mode, it is possible to perform also the spectroscopic analysis of the detected photons. Fig. 7(b) shows the raw data of a 2-D image of the brass mask with four holes (0.2 mm diameter) shown in Fig. 7(a) and collected by four

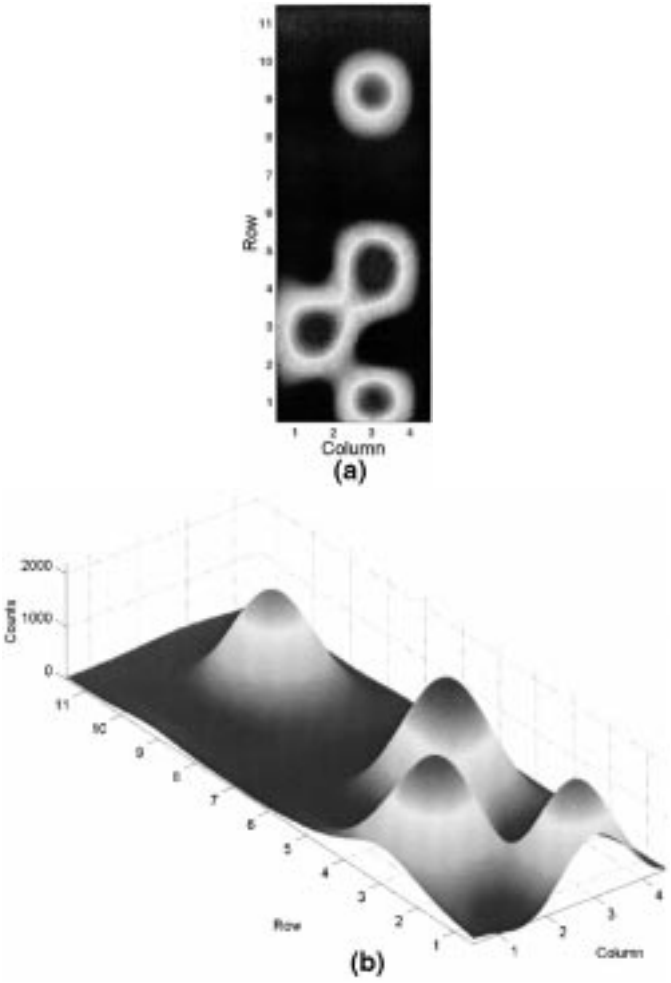

Fig. 8. Interpolation of the raw data of Fig. 7(b). (a) Gray plot. (b) Three-dimensional surface.

columns of 11 pixels each. By interpolating the raw data, we can accurately reconstruct the hole geometry, as shown in Fig. 8.

B. Measurements With Synchrotron Light

We have performed some imaging tests in the harsh environment of the SYRMEP beamline at ELETTRA Sincrotrone Trieste, Italy, taking benefit of the highly collimated beam that is available in a synchrotron facility. The measurement setup is very similar to that of Fig. 7(a). The imaged mask is shown in Fig. 9(a). As the mask is larger than the active area of the present prototype, the detector was panned to cover the whole mask. The energy of the incident beam was set to 15 keV. The image seen by the CDD is shown in Fig. 9(b). As can be noticed, the CDD is able to see the "X-RAY."

We have also imaged the metallic bolt screwed in a Teflon nut shown in Fig. 10(a). Fig. 10(b) shows the cross-section of the radiographed object. The bolt was scanned along its axis. The CDD was operated at 100-kHz frame frequency. The energy of the incident beam was set to 22 keV, high enough to pass through the Teflon nut. The image acquired by the CDD is shown in Fig. 11(a), while Fig. 11(b) shows the cubic interpolation of the raw data. The threads of the upper part of the bolt are clearly visible. The Teflon nut absorbs about 8/9 of the incident photons, as expected by calculating the attenuation given by 15 mm of Teflon. The smooth transition between air and Teflon is due to the 45° angle countersinking.

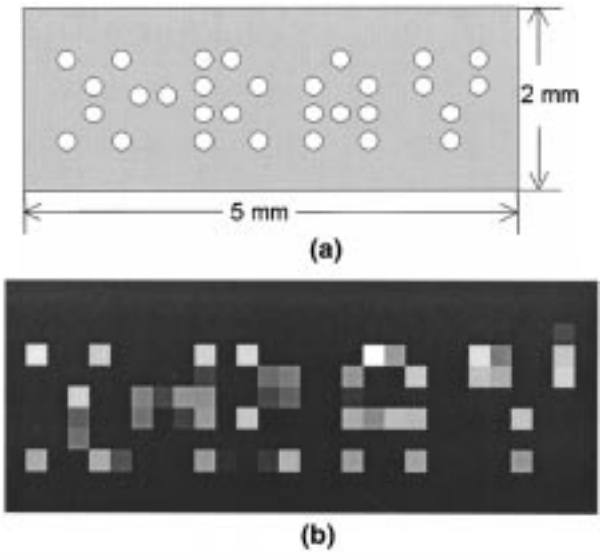

Fig. 9. (a) Brass mask layout. The mask is 0.3 mm thick, the holes' diameter is about 0.1 mm, and the holes' pitch is 0.3 mm. (b) Image of the mask shown in (a) as acquired by the CDD at ELETTRA Sincrotrone Trieste. The energy of the X-ray beam was 15 keV. The CDD was operated at 40-kHz frame frequency. The darker the pixel in the grayscale, the lower the number of counts in the pixel.

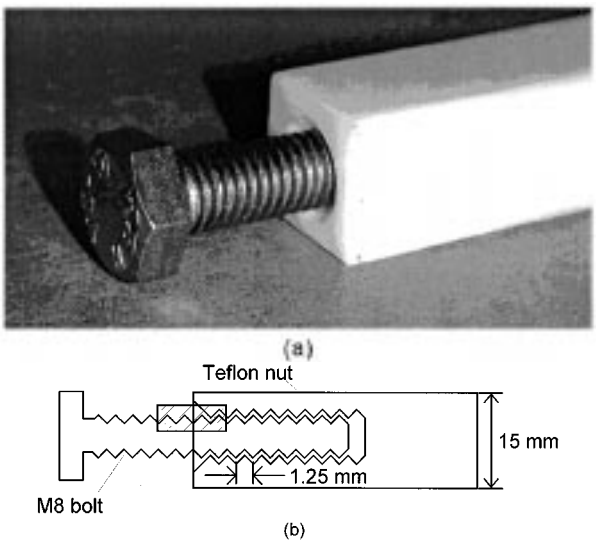

Fig. 10. (a) Photograph of the bolt in a Teflon nut. (b) Cross-section of the radiographed object. The scanned area (4.86×1.98 mm^2) is dashed.

IV. Conclusion

We have presented the first 2-D X-ray images acquired with controlled-drift detectors and shown their potentiality in energy-resolved X-ray imaging when operated at room temperature. We expect to obtain energy resolutions close to present state-of-the-art X-ray imagers with a Peltier-cooled controlled-drift detector system. This feature is of great interest for X-ray telescopes requiring high energy and time resolution onboard "light" space missions and for the development of compact measurement heads for scientific and industrial applications.

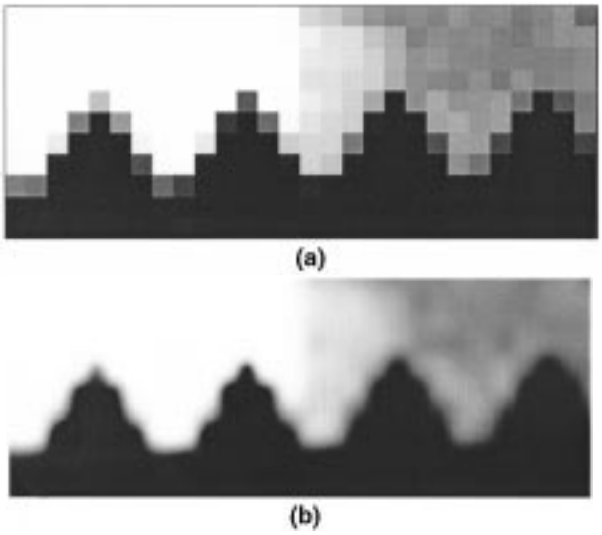

Fig. 11. (a) Radiography of the bolt in the Teflon nut shown in Fig. 10(b) as acquired by the CDD at ELETTRA Sincrotrone Trieste. The energy of the X-ray beam was 22 keV. The CDD was operated at 100-kHz frame frequency. The darker the pixel in the grayscale, the lower the number of counts in the pixel. The threads of the bolt are clearly visible. (b) Cubic interpolation of the raw data shown in (a).

ACKNOWLEDGMENT

The authors gratefully acknowledge E. Gatti for many fruitful discussions, P. Holl and the staff of the MPI Halbleiterlabor for the detector production and S. Kemmer for the careful bonding of the detector chip. A. Castoldi, A. Galimberti, and C. Guazzoni would like to thank R. Menk and F. Arfelli for the kind hospitality at the SYRMEP beamline (ELETTRA Sincrotrone Trieste).

REFERENCES

[1] "Controlled-drift apparatus for detecting energy and point of incidence of elecromagnetic radiations or ionizing particles," U.S. Patent 6 249 033, 2001.

[2] "Apparatus and method for detecting electromagnetic radiation or ionizing particles," Eur. Patent EP 0 862 226, 2001.

[3] A. Castoldi, C. Guazzoni, A. Longoni, E. Gatti, P. Rehak, and L. Strüder, "Conception and design criteria of a novel silicon device for the measurement of position and energy of X-rays," *IEEE Trans. Nucl. Sci.*, vol. 44, pp. 1724–1732, 1997.

[4] A. Castoldi, E. Gatti, C. Guazzoni, A. Longoni, P. Rehak, and L. Strüder, "The controlled-drift detector," *Nucl. Instrum. Methods*, vol. A439, pp. 519–528, 2000.

[5] L. Strüder, H. Bräuninger, U. Briel, R. Hartmann, G. Hartner, D. Hauff, N. Krause, B. Maier, N. Meidinger, E. Pfeffermann, M. Popp, C. Reppin, R. Richter, D. Stötter, J. Trümper, U. Weber, P. Holl, J. Kemmer, H. Soltau, A. Viehl, and C. v. Zanthier, "A 36 cm^2 large monolytic pn-charge coupled device X-ray detector for the european XMM satellite mission," *Rev. Sci. Instrum.*, vol. 68, pp. 4271–4274, 1997.

[6] A. Castoldi, C. Guazzoni, P. Rehak, and L. Strüder, "Spectroscopic-grade X-ray imaging up to 100 kHz frame rate with controlled-drift detectors," *IEEE Trans. Nucl. Sci.*, vol. 48, pp. 982–986, 2001.